Black Hole Accretion in Low States: Electron Heating

Siming Liu,[1] Christopher L. Fryer,[1,2] and Hui Li[1]

ABSTRACT

Plasmas in an accretion flow are heated by MHD turbulence generated through the magneto-rotational instability. The viscous stress driving the accretion is intimately connected to the microscopic processes of turbulence dissipation. We show that, in a few well-observed black hole accretion systems, there is compelling observational evidence of efficient electron heating by turbulence or collective plasma effects in low accretion states, when Coulomb collisions are not efficient enough to establish a thermal equilibrium between electrons and ions at small radii. However, charged particles reach a thermal equilibrium with their kind much faster than with others through Coulomb collisions, a two-temperature accretion flow is expected. We consider a Keplerian accretion flow with a constant mass accretion rate in the pseudo-Newtonian gravitational potential and take into account the bremsstrahlung, synchrotron, and inverse Comptonization cooling processes. The critical mass accretion rate, below which the two-temperature solution may exist, is determined by the cooling processes and the collisional energy exchanges between electrons and ions and has very weak dependence on the collision-less heating of electrons by turbulence, which becomes more important at lower accretion rates. Collision-less heating of electrons by MHD turbulence can no longer be ignored in quantitative investigations of these systems.

Subject headings: acceleration of particles — accretion, accretion disks — black hole physics — plasmas — radiation mechanisms: thermal— turbulence

1. Introduction

Black hole accretion is one of the most powerful energy sources in the universe. When the luminosity of the system is close to the Eddington luminosity, the accretion can be described by the classical Shakura-Sunyaev disk (1973), which produces a multi-color blackbody

[1]Los Alamos National Laboratory, Los Alamos, NM 87545; liusm@lanl.gov; hli@lanl.gov

[2]Physics Department, The University of Arizona, Tucson, AZ 85721; clfreyer@lanl.gov

radiation with the flux and temperature determined by the black hole mass and accretion rate. Observations of galactic black hole X-ray binaries strongly support such a scenario (Gierliński & Done 2004). The less energetic non-thermal high energy emission component frequently observed has been attributed to hot magnetized coronas above the disk (Gierliński et al. 1999; Zhang et al. 2000).

The magneto-rotational instability (MRI) has been generally accepted as the basic mechanism producing the less well-understood turbulence viscosity that drives the accretion (Balbus & Hawley 1991). The dissipated gravitational energy is first converted into MHD turbulence, which then heats the accretion flow through viscous and Ohmic dissipations. In these optically thick slim disks, the Coulomb collision time scales are much shorter than other relevant time scales, electrons and ions reach a thermal equilibrium so that the observed emission can be well-described with blackbody spectra modified by the radiation transfer through the disk structure. The acceleration and/or heating of electrons by turbulence can at most be studied with observations of the non-thermal component emitted from the collision-less coronas (Dermer et al. 1996; Li & Miller 1997).

Many black hole candidates are often observed in a super- or sub- Eddington emission state, and there are many distinct observational phenomena, such as relativistic outflows and quasi-periodic oscillations, that have not been well understood though many models have been proposed (Fender et al. 2004; Remillard et al. 1999; Falcke et al. 2004; Camenzind 2005). Both theoretical investigations and observations suggest that, below a critical mass accretion rate $\dot{M}_{\rm cr}$, a two-temperature accretion flow likely develop near the black hole due to the much higher radiation efficiency of electrons than ions and inefficient Coulomb coupling between them so that the local thermal equilibrium can not be established between the two (Shapiro et al. 1976; Rees et al. 1982; Zdziarski et al. 2002; Titarchuk & Fiorito 2004). Such a two-temperature flow is also expected due to the fact that charged particles reach a thermal equilibrium with their kind much faster than with others through Coulomb collisions (Spitzer 1962). This paper studies the electron heating processes in these low states.

Besides energy exchanges through Coulomb collisions, charged particles can also be energized by plasma waves through collision-less processes. These energization processes will directly affect the characteristics of the observed emission and therefore play crucial roles in our study of these systems in the low states. As pointed out by Bisnovatyi-Kogan and Lovelace (1997), the Ohmic heating of electrons through dissipation of MHD turbulence can be very efficient. Sharma et al. (2007) recently found that electrons might also be energized in the dynamo processes of magnetic field amplification through the MRI. However, the complexity of processes in a turbulent plasma has made the collision-less electron heating by collective plasma effects a difficult problem (Rees et al. 1982). In these theoretical investi-

gations, certain assumptions have to be made on the coupling between charged particles and the turbulent electromagnetic fields to derive some quantitative results, which are usually sensitive to the prior assumptions.

The collision-less electron heating by turbulent magnetic fields is often ignored in most phenomenological models (Shapiro et al. 1976). In the advection dominated accretion flow models, it is simply assumed that a small fraction of the energy dissipated through viscosity is converted into electrons (Esin et al. 1998; Yuan et al. 2006), suggesting that this is a trivial process. Alternatively, one-temperature models have been proposed for Sagittarius A*, the compact radio source associated with the low-luminosity supermassive black hole in the Galactic Center (Schödel et al. 2002; Ghez et al. 2005), assuming that electrons and protons are coupled by turbulence effectively (Melia et al. 2000, 2001).

On the other hand, the collision-less electron heating processes may be constrained by observations of the relevant systems. Recent studies of flares from Sagittarius A* indicate that electrons can be heated efficiently by MHD turbulence and the distribution of relativistic electrons under the influence of a turbulent magnetic field can be approximated as relativistic Maxwellian (Baganoff et al. 2001; Genzel et al. 2003; Gillessen et al. 2006; Bittner et al. 2007). The same processes may also play important roles in the heating of electrons in the two-temperature accretion flows. In this paper, we consider a Keplerian accretion disk model and the dominant cooling processes in a fully ionized magnetized plasma. We show that Coulomb collisions with ions can not heat electrons efficiently and an extra electron heating process is required to explain observations of Sagittarius A* and the galactic X-ray binary Cygnus X-1 (Wilms et al. 2006). This is in contradiction with what is suggested in some of the previous studies. Magnetic turbulence could play such a role, and we believe that the collision-less heating of electrons by MHD turbulence should not be ignored in any quantitative studies of these low accretion states.

The critical mass accretion rate is determined by the cooling processes and collisional energy exchanges between electrons and ions. Although the collision-less turbulence heating can reduce $\dot{M}_{cr}$ by increasing the radiation efficiency and cooling rate, we find that this effect is insignificant. More detailed investigations of the radiation spectrum and magneto-hydrodynamic processes are needed to study these plasma processes quantitatively.

The basic equations for the accretion disk are given in § 2. In § 3, we discuss the electron heating processes and show that observations of Sagittarius A* in the millimeter and sub-millimeter range are difficult to explain without introducing efficient electron heating by turbulence. The cooling processes are studied in §4 and the model is applied to galactic X-ray binaries in § 5. In § 6, we draw conclusions and discuss the model limitations and possible improvements in the future.

2. Basic Equations for Keplerian Flows in the Pseudo-Newtonian Potential

We consider a fully ionized hydrogen plasma. Then the gas pressure and the thermal energy density are given, respectively, by

$$P = nk_{\rm B}(T_p + T_e), \tag{1}$$

$$\mathcal{E} = nk_{\rm B}(1.5T_p + \alpha T_e), \tag{2}$$

where the gas density, the proton and electron temperatures are denoted by n, T_p and T_e, respectively, $k_{\rm B}$ is the Boltzmann constant, and $\alpha = x[3K_3(x) + K_1(x) - 4K_2(x)]/4K_2(x)$ with $x = m_e c^2/k_{\rm B}T_e$, where m_e and c denote the electron mass and the speed of light, respectively, and K_i refers to the ith order modified Bessel function. $K_i(x) \to 2^{i-1}(i-1)!/x^i$ as $x \to 0$ and $K_i(x) \to (\pi/2x)^{1/2}\exp(-x)[1 + (4i^2 - 1)/8x]$ as $x \to \infty$.

In the pseudo-Newtonian gravitational potential (Paczyńsky & Wiita 1980), the potential and Keplerian angular velocity are given, respectively, by

$$\phi = -\frac{GM}{r - r_{\rm S}}, \tag{3}$$

$$\Omega_{\rm K} = \left[\frac{GM}{r(r - r_{\rm S})^2}\right]^{1/2}, \tag{4}$$

where the gravitational constant, the black hole mass and the radius are denoted by G, M and r respectively, and $r_{\rm S} = 2GM/c^2$ is the Schwarzschild radius of the black hole.

Due to the decoupling between electrons and ions, the radiation efficiencies of two-temperature accretion flows will not be as high as the optically thick slim disks. The accretion processes likely drive strong winds from the hot disk (Blandford and Begelman 1999), and there are currently no strong observational constraints on these processes. To simplify our model we consider the steady state properties of the accretion flow averaged in the vertical direction and assume a radius independent accretion rate, i.e., ignoring the effects of winds:

$$\dot{M} = -4\pi r H v_r n(m_p + m_e), \tag{5}$$

where v_r and H are the radial velocity and the scale height of the accretion flow, respectively, and m_p is the proton mass. The vertical structure of the disk can be very complicated as suggested by MHD simulations (Hawley & Balbus 2002) and may be essential to explain the observed non-thermal high energy emission in low states (Dermer et al. 1996; Li & Miller 1997). It, however, is not expected to introduce significant changes to our quantitative results below, which deal with the energetically dominant thermal emission component from the main body of the hot accretion flow (Shapiro et al. 1976).

Following Blandford and Begelman (1999), we assume that the angular momentum flux through the disk is negligible, which is also expected for strongly magnetized disks (Agol & Krolik 2000). MHD simulations also show that the azimuthal velocity of the flow is given by the Keplerian velocity $v_K = r\Omega_K$ (Hawley & Balbus 2002), which requires the inner boundary radius $r_i \geq 3\,r_S$, the radius of the last stable orbit. From the angular momentum conservation of the accretion flow, we then have

$$v_r = \nu \frac{\mathrm{d}\ln\Omega_K}{\mathrm{d}r} = -\nu\left(\frac{1}{2r} + \frac{1}{r - r_S}\right) \tag{6}$$

where the kinematic viscosity

$$\nu = \frac{2\beta_p\beta_\nu k_B(T_p + T_e)(r - r_S)^2 r^{1/2}}{(m_p + m_e)(3r - r_S)(GM)^{1/2}}, \tag{7}$$

and in accord with Melia et al. (2001) $\beta_p = \langle B^2\rangle/8\pi P$ and β_ν is defined as the ratio of the total stress to the magnetic field energy density $\langle B^2/8\pi\rangle$.[1] Then the radial velocity can be rewritten as

$$v_r = -\frac{\beta_\nu\beta_p k_B(T_p + T_e)(r - r_S)}{(m_p + m_e)(GMr)^{1/2}}. \tag{8}$$

Since the magnetic field is dominated by the toroidal component, one has

$$H = \left[\frac{r k_B(T_p + T_e)(1 + 2\beta_p)}{GM(m_p + m_e)}\right]^{1/2}(r - r_S), \tag{9}$$

$$n = \frac{GM\dot{M}(m_p + m_e)^{1/2}}{4\pi\beta_\nu\beta_p[k_B(T_p + T_e)]^{3/2}(1 + 2\beta_p)^{1/2}r(r - r_S)^2}. \tag{10}$$

The energy conservation equation is given by

$$\frac{\mathrm{d}}{Hr\mathrm{d}r}\left\{Hrv_r[P(1 + 2\beta_p) + \mathcal{E} + n(m_p + m_e)[\phi - 0.5v_K^2 + 0.5v_r^2]]\right\} = -\Lambda, \tag{11}$$

where Λ is the radiative cooling rate, and we have ignored any energy fluxes carried away from the disk by winds and waves and taken into account the effects of magnetic fields properly (Melia et al. 2001). Note that the work done by the torque force is given by $-\mathrm{d}[Hrv_r n(m_p + m_e)v_K^2]/\mathrm{d}r$. Then we have

$$\frac{\mathrm{d}}{\mathrm{d}r}\varepsilon = -\frac{\Lambda}{v_r n}, \tag{12}$$

---

[1]Note that the viscous parameter in the classical disk model $\alpha = \beta_\nu\beta_p/(1 + 2\beta_p)$.

where

$$\varepsilon = k_{\mathrm{B}}[T_e(\alpha + 1 + 2\beta_p) + T_p(2.5 + 2\beta_p)] + (m_p + m_e)[\phi - 0.5v_{\mathrm{K}}^2 + 0.5v_r^2] \qquad (13)$$

can be considered as the energy of the accretion flow per proton and $\dot{M}\varepsilon/m_p$ gives the outwardly directed energy flux through the accretion disk (Blandford & Begelman 1999).

3. Electron Heating

Because the viscous stress driving the accretion is induced by the MRI (Balbus & Hawley 1991), the gravitational energy dissipation first generates MHD turbulence, which then heats the gas as the turbulence cascades from large scales to small scales. A fraction of the turbulence energy may also be carried away from the disk by MHD waves propagating toward large radii. However, this process is not expected to dominate the dynamics of the accretion flow at least for the relative more powerful states, when the hard X-ray luminosity of X-ray binaries can be a significant fraction of the Eddington luminosity. Very high accretion rates will be needed to produce the observed X-ray power if waves carry most of the dissipated gravitational energy toward large radii. The turbulence cascade also needs to be suppressed dramatically to make the wave escape process dominant. Therefore, in the steady state, the viscous heating rate

$$\Gamma = v_r n(m_p + m_e)\frac{\mathrm{d}[-\phi + 0.5v_{\mathrm{K}}^2]}{\mathrm{d}r}$$

should be slightly greater than the turbulence cascade rate

$$\Gamma_B = \frac{C_2 c_S B^2}{8\pi H},$$

where $C_2 \sim 1$ is dimensionless and determined by the properties of the turbulence and

$$c_S = \left[\frac{k_{\mathrm{B}}(T_i + T_e)(1 + 2\beta_p)}{m_p + m_e}\right]^{1/2}$$

is the speed of fast mode waves (Liu et al. 2006b). There is therefore an intimate connection between the viscous stress and turbulence dissipation. It is, however, not clear how this energy is distributed between electrons and protons in a collision-less plasma and what determines this energy partition, especially for hot plasmas in the two-temperature accretion flow of black holes. In the following, we will show how observations of low states of black hole accretion systems may be used to constrain the collision-less electron heating rate by turbulence.

The disk structure can be obtained once one specifies the electron heating and cooling rates and the electron and proton temperatures at the outer boundary. Following Blandford and Eichler (1987), we have the electron heating time by turbulence (Liu et al. 2006b)

$$\tau_{\mathrm{ac}} = \frac{3C_1 H \langle v_e \rangle}{c_S^2} \, , \tag{14}$$

where C_1 is a dimensionless constant, and

$$\langle v_e \rangle = \frac{2c(x+1)}{x^2 K_2(x) \exp(x)}$$

is the mean electron speed. Note that $\langle v_e \rangle / c \to (8k_{\mathrm{B}} T_e / \pi m_e c^2)^{1/2}$ as $x \to \infty$ and the electron heating becomes relatively more efficient at smaller radii if electrons become relativistic and $\langle v_e \rangle$ approaches to c. Then we have

$$\frac{\mathrm{d}T_e}{\mathrm{d}r} = \frac{T_e}{\tau_{\mathrm{ac}} v_r} + \frac{T_p - T_e}{\tau_{\mathrm{Coul}} v_r} - \frac{\Lambda}{n \alpha k_{\mathrm{B}} v_r} \, , \tag{15}$$

where

$$\tau_{\mathrm{Coul}} = \frac{3\pi m_e m_p \langle v_e \rangle^3}{256 n e^4 \ln \lambda} \, ,$$

is the electron-proton energy exchange time through Coulomb collisions, e is the elemental charge unit, and $\ln \lambda \simeq 15$ for most astrophysical situations (Spitzer 1962).

There are several ways to estimate C_1. For a non-radiative accretion flow, $\Lambda = 0$. At large radii, we can ignore the kinetic energy associated with the radial motion and $\alpha = 1.5$. If we ignore the Coulomb coupling term, we have the following solution:

$$
\begin{aligned}
c_S &= (k_{\mathrm{B}}(T_e + T_p)(1 + 2\beta_p)/(m_p + m_e))^{1/2} = [3(1 + 2\beta_p)/(5 + 4\beta_p)]^{1/2} v_{\mathrm{K}} \,, &(16)\\
H &= [3(1 + 2\beta_p)/(5 + 4\beta_p)]^{1/2} r \,, &(17)\\
v_r &= -[3\beta_\nu \beta_p/(5 + 4\beta_p)] v_{\mathrm{K}} \,, &(18)\\
n &= [3/(5 + 4\beta_p)]^{-3/2}(1 + 2\beta_p)^{-1/2} \dot{M}/4\pi \beta_\nu \beta_p (m_p + m_e) r^2 v_{\mathrm{K}} \,, &(19)\\
k_{\mathrm{B}} T_e &= [3/(5 + 4\beta_p)(1 + 2\beta_p)]^{-1}[\pi/72 C_1^2 \beta_\nu^2 \beta_p^2] m_e v_{\mathrm{K}}^2 \,, &(20)\\
T_p/T_e &= [3/(5 + 4\beta_p)]^2 [72 C_1^2 \beta_\nu^2 \beta_p^2/\pi(1 + 2\beta_p)](m_p + m_e)/m_e - 1 \\
&= 1.5 \times 10^4 [C_1 \beta_\nu \beta_p/(1 + 0.8\beta_p)]^2/(1 + 2\beta_p) - 1 \,. &(21)
\end{aligned}
$$

Then we have

$$C_1 = 8.1 \times 10^{-3}[(T_p/T_e + 1)(1 + 2\beta_p)]^{1/2}(1 + 0.8\beta_p)/\beta_\nu \beta_p > 8.1 \times 10^{-3}(1 + 2\beta_p)^{1/2}(1 + 0.8\beta_p)/\beta_\nu \beta_p \,.$$

It is interesting to note that the proton temperature satisfies an equation similar to equation $(15)^2$:

$$\frac{dT_p}{dr} = \frac{T_p}{\tau_{ac} v_r},$$

suggesting that the heating time of protons is the same as electrons. Since the mean speed of protons $\langle v_p \rangle$ is usually different from $\langle v_e \rangle$, it is likely that the dimensionless constant C_1, which is determined by the microscopic physics of resonant and/or non-resonant coupling between particles and turbulence, is different for protons and electrons. Otherwise, $T_p/T_e = m_p/m_e$, and we have

$$C_1 = [(5 + 4\beta_p)/18\beta_\nu \beta_p][\pi(1 + 2\beta_p)/2]^{1/2} . \tag{22}$$

For this solution, the Coulomb energy exchanges between electrons and protons (with τ_{Coul} independent of the radius r) become relatively more important at larger radii. So we have a one-temperature flow at large radii, which develops into the above solution at the radius, where the Coulomb energy exchange time becomes comparable to the accretion time:

$$\tau_{\mathrm{vis}} \equiv -r/v_r \simeq \frac{(5 + 4\beta_p)r^{3/2}}{3\beta_\nu \beta_p (GM)^{1/2}} . \tag{23}$$

The transition radius is therefore given by

$$
\begin{aligned}
r_t/r_S &= \left(\frac{\pi^2 m_e m_p (m_p + m_e) GM c^3 [1 + 2\beta_p]^2}{3[5 + 4\beta_p]2^{15/2} e^4 \ln \lambda C_1^3 \beta_\nu \beta_p \dot{M}} \right)^{2/3} = \left(\frac{\pi^2 m_p [1 + 2\beta_p]^2}{45[1 + 0.8\beta_p]2^{13/2} m_e \ln \lambda C_1^3 \beta_\nu \beta_p} \frac{L_{\mathrm{Edd}}}{\dot{M} c^2} \right)^{2/3} \\
&\simeq \left(\frac{0.3[1 + 2\beta_p]^2}{[1 + 0.8\beta_p]C_1^3 \beta_\nu \beta_p} \frac{L_{\mathrm{Edd}}}{\dot{M} c^2} \right)^{2/3} \simeq 3.4 \times 10^3 \left(\frac{\beta_\nu^4 \beta_p^4 [1 + 2\beta_p]}{[1 + 0.8\beta_p]^8} \right)^{1/3} \left(\frac{L_{\mathrm{Edd}}}{\dot{M} c^2} \right)^{2/3} ,
\end{aligned}
\tag{24}
$$

where $L_{\mathrm{Edd}} = 4\pi GM(m_p + m_e)c/\sigma_T$ is the Eddington Luminosity and $\sigma_T = (8\pi/3)e^4/m_e^2 c^4$ is the Thomson scattering cross-section, and we have used the above solution to obtain the electron temperature and assumed $T_e = T_p$ to get the last expression. We see that two-temperature flows can readily develop at small radii even without considering the electron cooling processes.

When Coulomb collisions become less efficient at smaller radii, in principle the distributions of electrons and protons are not necessarily Maxwellian. However, at a given mean energy, the time scales for protons and electrons reaching equilibrium with themselves are,

---

[2]With the assumptions adopted above, this equation actually can be derived from equations (11) and (15). It is therefore not an independent equation.

respectively, $\sim (m_e/m_p)^{1/2}\tau_{\text{Coul}}$ and $\sim (m_e/m_p)\tau_{\text{Coul}}$, which are much shorter than τ_{Coul}, the time scale for electrons and protons reaching thermal equilibrium with each other (Spitzer 1962). The electron and proton distributions therefore may start to deviate from Maxwellian at $(m_e/m_p)^{2/3}r_t$ and $(m_e/m_p)^{1/3}r_t$, respectively. So the transition radius, where the proton distribution may deviate from Maxwellian, is more than ten times smaller than the radius, where the two-temperature flow starts to develop. The transition radius for electrons is even smaller, and a Maxwellian distribution can be achieved at small radii through relativistic effects and cooling processes (Wolfe & Melia 2006; Bittner et al. 2007). We therefore expect that the electron distribution be always dominated by a thermal component and, over a significant radius range, a two-temperature flow develop self-consistently. The fact that the low-hard state spectra of X-ray binaries can be fitted with the thermal inverse Comptonization model also suggests a dominant thermal electron component.

At very low accretion rates, the Coulomb collision time scales can be much longer than other relevant time scales near the black hole, and we do not expect Maxwellian distributions for both electrons and ions. This is a completely new regime, where the behavior of the turbulent plasma has not been well studied. In these cases, the "temperature" of the particles should be interpreted as a measurement of their mean energies. The actual electron distribution may be constrained by studying its radiation spectrum. We note that the proton distribution is always expected to deviate from Maxwellian at very small radii, where the energy dissipation rate is high, and a high energy proton population may be responsible for the formation of jets in the low states (Dermer et al. 1996; Liu et al. 2006a). A detailed investigation of these effects is beyond the scope of this paper.

From $\Gamma > \Gamma_B$ and the above solution, we have $\beta_\nu > 2C_2/3$. The viscous stress therefore needs to be comparable to the turbulent magnetic field energy density. Since the viscous stress should not be much greater than the turbulent magnetic field energy density (Pessah et al. 2006), the fact that $C_2 \sim 1$ requires that Γ_B can not be much less than Γ. So the energy carried away by winds and/or waves should account for a small fraction of the dissipated gravitational energy except that the turbulence cascade from large scales to small scales is suppressed for some reason so that C_2 becomes much less than 1.

We also note that for this solution, $\tau_{\text{ac}} \propto r^{3/2}$. The turbulence electron heating effectively converts a constant fraction δ of the viscously dissipated gravitational energy into the internal energy of electrons. The electron heating rate by turbulence is given by $\alpha n k_{\text{B}} T_e/\tau_{\text{ac}}$. Then

$$\delta \simeq [\pi(5 + 4\beta_p)(1 + 2\beta_p)/216C_1^2\beta_\nu^2\beta_p^2]m_e/(m_p + m_e) < 1$$

gives $C_1\beta_\nu\beta_p > 6.3 \times 10^{-3}[(1 + 0.8\beta_p)(1 + 2\beta_p)]^{1/2}$. Although this result is similar to that proposed in the advection dominated accretion flow models (Esin et al. 1998), the electron heating studied here becomes very efficient when cooling reduces the electron temperature or

the electrons become relativistic since the heating time is proportional to the mean velocity of electrons. Accordingly, Coulomb collisional heating may suppress the turbulence heating by increasing $\langle v_e \rangle$.

Since the heating is more efficient when electrons become relativistic, an even stricter constraint on C_1 can be obtained by considering the accretion processes at small radii. For $\Lambda = 0$ and $T_e \gg T_p$, $\alpha = 3$, the accretion time is given by

$$\tau_{\text{vis}} \equiv -r/v_r \simeq \frac{(8 + 4\beta_p)r^{3//2}}{3\beta_\nu\beta_p(GM)^{1/2}} \, . \tag{25}$$

To avoid electrons being overheated, the electron heating time needs to be longer than the accretion time, then we have:

$$C_1\beta_\nu\beta_p > \left(\frac{8 + 4\beta_p}{27}\right)^{1/2} \left(\frac{GM}{rc^2}\right)^{1/2} < 0.3 \, , \tag{26}$$

where we have used the fact that, for the accretion flow we are considering, $r > 3r_{\text{S}}$.

For $\Lambda = 0$, we solve equations (12) and (15) numerically to constrain the heating rate more quantitatively. For $\beta_p = 1$, we find that $C_1\beta_\nu\beta_p$ needs to be greater than 0.15 to avoid the proton temperature decreasing below zero at small radii at certain accretion rates due to efficient electron heating. Panel "a" of Figure 1 shows the temperature profiles for $\dot{M} = 10^{-7}, 10^{-3}, 10L_{\text{Edd}}/c^2$. (Note that the Eddington accretion rate is usually defined as $\dot{M}_{\text{Edd}} \equiv 10L_{\text{Edd}}/c^2$.) The other model parameters $C_1 = 1.5$, $\beta_\nu = 0.1$, $\beta_p = 1$, and $T_e = T_p = GMm_p/10k_Br_o$ at the outer boundary $r_o = 10^4r_{\text{S}}$. When $\dot{M}$ is small, Coulomb collision effects are negligible. We recover the solution given by equations (16—21) at large radii. At small radii, the electron temperature goes beyond that given by equation (20) due to the relativistic effect discussed above. With the increase of $\dot{M}$, the electron and proton temperatures become closer to each other at larger radii. At small radii, because of efficient heating of relativistic electrons, the electron temperature is higher than the proton temperature for $\dot{M} = 10^{-3}L_{\text{Edd}}/c^2$. When the accretion rate becomes comparable to or higher than the Eddington accretion rate $\sim 10L_{\text{Edd}}/c^2$, the electron and proton temperatures become identical due to very efficient Coulomb collisions.

The linearly polarized millimeter and sub-millimeter emission from Sagittarius A* (Aitken et al. 2000; Schödel et al. 2002; Ghez et al. 2005) reveals a mass accretion rate below $10^{-5}L_{\text{Edd}}/c^2$ (Quataert & Gruzinov 2000). X-ray observations and detailed modeling suggest an even lower accretion rate (Baganoff et al. 2001; Melia et al. 2000; Liu & Melia 2002). VLBI observations have shown that this emission comes from a region within $\sim 15 \, r_{\text{S}}$ of the black hole and should originate from a hot accretion torus (Shen 2005; Melia et al. 2001). The dotted line in Panel "a" of Figure 1 shows the electron (lower) and proton (upper)

temperature profiles for $\dot{M} = 10^{-5}L_{\mathrm{Edd}}/c^2$ and $C_1 = 15$, which is ten times bigger than that for the other lines, giving much less efficient electron heating by turbulence. Although we have adopted a relatively high accretion rate, Coulomb collisions are not efficient enough to heat electrons to relativistic energies required to produce the observed synchrotron emission. A fit to the millimeter and sub-millimeter spectrum and polarization gives $C_1\beta_\nu\beta_p \simeq 0.1$, which is comparable to the maximum heating rate discussed above, where cooling is absent, and is more than 10 times smaller than that given by equation (22) (Liu et al. 2007). One can show that C_1 for electrons is more than 10 times smaller than that for protons in this case. This could be due to the high mean momentum of protons so that the action of protons on turbulence in their stochastic scattering processes is important. The proton heating is then suppressed giving rise to a more than 10 times longer acceleration time than electrons at a given mean speed of both particles.

4. Electron Cooling

For a fully ionized magnetized plasma, synchrotron, inverse Comptonization (IC), and bremsstrahlung are the dominated emission mechanisms (Rybicki & Lightman 1979). In the low accretion states of black holes, the disk is optically thin to bremsstrahlung radiation. We therefore have the bremsstrahlung cooling rate

$$\Lambda_{\mathrm{brem}} = \left(\frac{2\pi k_B T_e}{3m_e}\right)^{1/2}\frac{32\pi e^6}{3hm_ec^3}n^2 g_{\mathrm{B}} = 1.4\times 10^{-27}T_e^{1/2}n^2 g_{\mathrm{B}}\,, \tag{27}$$

where $g_{\mathrm{B}} \simeq 1.2$ is the Gaunt factor and h is the Planck constant. For equations (16)-(21), $\Lambda_{\mathrm{brem}} \propto r^{-7/2}$ and the bremsstrahlung cooling time of electrons $\tau_{\mathrm{bc}} = \alpha k_B n T_e/\Lambda_{\mathrm{brem}} \propto r$. Including this energy loss process, we find that the disk collapses to a low temperature flow toward small radii when $\dot{M} > \dot{M}_{\mathrm{cr}} = 2.63\times 10^{-2}L_{\mathrm{Edd}}/c^2$ for an outer boundary radius of $10^4 r_{\mathrm{S}}$. This can be understood by comparing τ_{bc} with the accretion time $\tau_{\mathrm{vis}} \propto r^{3/2}$ [See eq. (23)]. Then we have

$$\dot{M}_{\mathrm{cr}} = \frac{3\sqrt{3m_p/\pi m_e}h\beta_\nu^2\beta_p^2 v_{\mathrm{K}}}{8e^2 g_{\mathrm{B}}}\left(\frac{3}{5+4\beta_p}\right)^3\frac{L_{\mathrm{Edd}}}{c^2} \simeq 2.9(r_{\mathrm{S}}/r)^{1/2}\frac{L_{\mathrm{Edd}}}{c^2}\,, \tag{28}$$

where we have assumed that $T_e = T_p$, i.e. $C_1 = [(5+4\beta_p)/18\beta_\nu\beta_p][\pi(1+2\beta_p)m_e/(m_e+m_p)]^{1/2}$, and used the model parameters for Panel "a" of Figure 1 to obtain the last expression. The critical mass accretion rate decreases with the increase of the outer boundary radius.

Panel "b" of Figure 1 shows the temperature profiles for several values of $\dot{M}$. The other model parameters are the same as Panel "a". Note that the bremsstrahlung cooling has little

effect on the temperature profile for $\dot{M} \ll \dot{M}_{\mathrm{cr}}$ because, compared with the accretion time given by equation (23), this cooling becomes less important toward smaller radii. For $\dot{M} = \dot{M}_{\mathrm{cr}}$, we see that the temperatures are lowered by the cooling near the outer boundary. Since the cooling rate is proportional to the density square, the cooling time scale is proportional to M, and $\dot{M}_{\mathrm{cr}} c^2 / L_{\mathrm{edd}}$ is independent of M. Pair production will increase the cooling rate and decrease $\dot{M}_{\mathrm{cr}}$. These results are similar to those given by Narayan & Yi (1995) though electron heating by turbulence has been included in our calculations, implying that the collision-less electron heating does not affect the bremsstrahlung cooling rate at large radii significantly.

One may define a critical radius with equation (28):

$$r_{\mathrm{cr}}/r_S = \frac{27 m_p h^2 \beta_\nu^4 \beta_p^4 c^2}{128 \pi m_e e^4 g_{\mathrm{B}}^2} \left(\frac{3}{5 + 4\beta_p} \right)^6 \left(\frac{L_{\mathrm{Edd}}}{\dot{M} c^2} \right)^2 \simeq 8.4 \left(\frac{L_{\mathrm{Edd}}}{\dot{M} c^2} \right)^2 . \tag{29}$$

A hot accretion flow can only exist below r_{cr}. When the transition radius r_t given by equation (24) is greater than r_{cr}, as is the case for relatively high accretion rates, a hot two-temperature flow may develop below r_{cr}. For low accretion rates, r_{cr} can be much greater than r_t, we have a hot one-temperature flow between r_t and r_{cr}, which develops into a hot two-temperature flow below r_t. The thin lines in Panel "b" corresponds to this case, where $r_t \sim 10^3 r_S$ and $r_{\mathrm{cr}} = 10^4 r_S$. From $r_t = r_{\mathrm{cr}}$, we have $\dot{M} c^2 / L_{\mathrm{Edd}} \simeq 156 \beta_\nu^2 \beta_p^2 / (1 + 2\beta_p)^{1/4}(1 + 0.8\beta_p)^{5/2}$ and $r_t = r_{\mathrm{cr}} \simeq 117 r_S (1 + 2\beta_p)^{1/2}/(1 + 0.8\beta_p)$. However, how exactly the hot flow may develop toward small radii is still an open question, which may depend on the nature of the large-scale flow and the coupling between the disk and its corona (Meyer-Hofmeister et al. 2005).

When the source is optically thin to synchrotron radiation, the cooling rate is given by

$$\Lambda_{\mathrm{syn}} = \frac{4e^4 n}{9 m_e^4 c^5} \langle p^2 \rangle B^2 \simeq 1.06 \times 10^{-15} n B^2 \frac{3x^2 + 12x + 12}{x^3 + x^2}, \tag{30}$$

where $\langle p^2 \rangle$ is the mean momentum square of the electrons (Melia & Coke 1999). For equations (16)-(21) and $x \ll 1$, $\Lambda_{\mathrm{syn}} \propto r^{-6}$. The corresponding cooling time scale $\tau_{\mathrm{sc}} \propto r^{7/2}$, which is more important at smaller radii. For $x \gg 1$, $\Lambda_{\mathrm{syn}} \propto r^{-5}$ and $\tau_{\mathrm{sc}} \propto r^{5/2}$. However, most of the thermal synchrotron emission is emitted at

$$\nu_E \simeq \frac{x + 20}{x + 1} \nu_c = \frac{60(1 + 0.05x)eB\gamma_c^2}{4\pi(x + 1)m_e c} = 8.4 \times 10^7 B\gamma_c^2 (1 + 0.05x)/(x + 1) \,\mathrm{Hz} ,$$

where $\gamma_c = 1/x + 1$ (Liu et al. 2006). The thermal synchrotron emission (emissivity per solid angle) and absorption coefficients are given, respectively, by (Petrosian 1981; Mahadevan, Narayan, & Yi 1996)

$$\mathcal{E}_\nu = \frac{\sqrt{3}e^3 \langle p^2 \rangle (x + 1)}{8\pi m_e^3 c^4 \langle \gamma^2 \rangle (1 + 0.19x)} B \, n \, z_M \, I(z_M) , \tag{31}$$

$$\kappa_\nu = \frac{\mathcal{E}_\nu c^2 [\exp{(h\nu/k_{\rm B}T_e)} - 1]}{2h\nu^3} \simeq \frac{\pi e n \langle p^2 \rangle}{3\sqrt{3}\gamma_c^4 m_e \langle \gamma^2 \rangle B k_{\rm B} T_e} \frac{I(z_M)(x+1)}{z_M(1+0.19x)} \,. \qquad (32)$$

where $\langle \gamma^2 \rangle \simeq (x+12)(x+1)/x^2$ is the mean Lorentz factor square of electrons, $(x+1)/(1+0.19x)$ is chosen to take into account the non-relativistic effects (see below), and

$$I(z_M) = 4.0505 z_M^{-1/6}(1 + 0.40 z_M^{-1/4} + 0.5316 z_M^{-1/2}) \exp(-1.8899\, z_M^{1/3}) \,, \qquad (33)$$
$$z_M = \nu/\nu_c \equiv 4\pi m_e c \nu/3eB\gamma_c^2 \,. \qquad (34)$$

We then have the optical depth through the emission region

$$\tau_\nu(\nu) \equiv \kappa_\nu(\nu)H = \frac{\pi e \langle p^2 \rangle n\ H}{3\sqrt{3}m_e \langle \gamma^2 \rangle k_{\rm B} T_e \gamma_c^4 B} \frac{I(z_M)(x+1)}{z_M(1+0.19x)} \,, \qquad (35)$$

which, for a given z_M, is proportional to $r^{23/4}$ for equations (16)-(21) and $x \ll 1$ and proportional to $r^{3/4}$ for $x \gg 1$. When $\tau_\nu(\nu_E)$ becomes greater than unity at large radii, one has to take into account the self-absorption effects. The corresponding synchrotron cooling rate may be approximated as

$$\begin{aligned}
\Lambda_{\rm syn} &= \frac{16\sqrt{3}\pi^2 k_{\rm B} T_e \nu_E^3}{45^2 I[(x+20)/(x+1)]c^2 H} \frac{\langle \gamma^2 \rangle (1+x)(1+0.19x)}{\gamma_c^2(1+0.05x)^2} \\
&= \frac{80\sqrt{3}e^3 k_{\rm B}}{3\pi I[(x+20)/(x+1)]m_e^3 c^5} \frac{T_e B^3 \langle \gamma^2 \rangle \gamma_c^4 (1+0.05x)(1+0.19x)}{H(x+1)^2} \\
&\simeq 6.4 \times 10^{-13} \frac{T_e B^3}{H} \frac{(x+12)(x+1)^3(1+0.05x)(1+0.19x)I(20)}{x^6 I[(x+20)/(x+1)]} \,, \qquad (36)
\end{aligned}$$

where the numerical factor is chosen so that the cooling rates given by equations (30) and (36) are equal when $\tau_\nu(\nu_E) = 1$, and $\Lambda_{\rm syn} \simeq 8\pi k_{\rm B} T_e \nu_E^3/3c^2 H$ for $x \gg 1$. That is, for cyclotron radiation in the optically thick regime, we assume a black body spectrum cutting off at $\nu_E = \nu_c$. This cooling is important at small radii since $\Lambda_{\rm syn} \propto r^{-47/4}$ and $\tau_{\rm sc} \propto r^{37/4}$ for equations (16)-(21) and $x \ll 1$. For $x \gg 1$, $\Lambda_{\rm syn} \propto r^{-23/4}$ and $\tau_{\rm sc} \propto r^{13/4}$.

We will assume that the IC is in the Thomson limit and the seed photons for IC are provided by the synchrotron radiation. Then we have the total cooling rate

$$\begin{aligned}
\Lambda &= \Lambda_{\rm syn} + \Lambda_{\rm IC} + \Lambda_{\rm brem} = \Lambda_{\rm syn}[1 + 8\pi(\Lambda - \Lambda_{\rm brem})H/cB^2] + \Lambda_{\rm brem} \qquad (37) \\
&= \Lambda_{\rm syn}(1 - 8\pi\Lambda_{\rm syn}H/cB^2)^{-1} + \Lambda_{\rm brem} \,.
\end{aligned}$$

Panel "c" of Figure 1 shows the temperature profiles with the above cooling processes included for $M = 3.4 \times 10^6 M_\odot$. The model parameters are the same as Panel "b" except $\dot{M} = 2.63 \times 10^{-6}$ (thick), 2.63×10^{-4} (medium), 2.63×10^{-2} (thin) $L_{\rm Edd}/c^2$. We note that

the electron temperature never goes above $\sim 10^{11}$ K, which may provide an alternative explanation to the observed upper limit in brightness temperature of powerful extragalactic radio sources (Readhead 1994). The critical mass accretion rate $\dot{M}_{cr} = 2.63 \times 10^{-2} L_{Edd}/c^2$ is the same as that obtained above, where only the bremsstrahlung cooling is considered. This is consistent with the fact that the synchrotron and IC coolings are unimportant at large radii. At small radii, these cooling processes do reduce the electron temperature.

Because the synchrotron cooling rate in the optically thick regime is proportional to $n^{3/2}/H$, the cooling time is proportional to $M^{3/2}$. This cooling becomes relatively more efficient for smaller black holes so that the electron temperature decreases with the decrease of M for given $\dot{M}c^2/L_{Edd}$. $\dot{M}_{cr}$ also decreases slightly with the decrease of M. For $M = 3.4 M_\odot$, we find $\dot{M}_{cr} = 2.13 \times 10^{-2} L_{Edd}/c^2$. Panel "d" of Figure 1 is the same as Panel "c" except that $M = 3.4 M_\odot$. The flatten part of the electron temperature in the inner region for $\dot{M} \sim \dot{M}_{cr}$ is dominated by Coulomb collisional heating and optically thick synchrotron cooling, which is very sensitive to the electron temperature when $x < 1$. We therefore expect that, for $\dot{M} = \dot{M}_{cr}$, the intrinsic brightness temperatures for extragalactic radio sources are higher for bigger black holes and there should be a correlation between the brightness temperature and the source luminosity. Pair production effects need to be incorporated to give more quantitative predictions.

Due to the low radiation efficiency at large radii, the critical mass accretion rate is not very sensitive to the electron heating rate either. Panel "e" of Figure 1 show the temperature profiles for $C_1 = 15$. The other parameters are the same as Panel "d", and $\dot{M}_{cr} = 2.51 \times 10^{-2} L_{Edd}/c^2$.

5. Application to X-ray Binaries in the Low-Hard States

It has been suggested that Coulomb collisions are efficient enough to heat electrons to explain observations of galactic X-ray binaries in the low-hard states (Shapiro et al. 1976; Esin et al. 1998). Although some of the relevant models may achieve an electron temperature in line with observations by adjusting parameters describing the source structure and/or dissipation processes, the related assumptions are not well justified both theoretically and observationally. It is also not obvious whether these models can explain the recently observed anti-correlation between the electron temperature and the Thomson optical depth of Cygnus X-1 over a large dynamical range (Wilms et al. 2006). The model proposed here is self-consistent and has the basic parameters to describe the dynamics and radiative processes. It is therefore well positioned to uncover new physical processes when applied to specific observations.

With the parameters adopted above, the model clearly can not explain the high hard X-ray luminosities observed in some of the galactic X-ray binaries. The hard X-ray luminosity can be a significant fraction of L_{Edd} for some sources. A much higher $\dot{M}_{\mathrm{cr}}$ is needed to produce such a high luminosity. To increase $\dot{M}_{\mathrm{cr}}$, one may increase the viscosity by increasing β_ν or decrease the outer boundary radius. The virial temperature at $r = 10^4 r_{\mathrm{S}}$ is already a few tens of keV, and we are interested in showing how electrons reach this temperature range from a large-scale cool accretion flow. We will consider the first option and set the outer boundary temperature $k_{\mathrm{B}}T_e = k_{\mathrm{B}}T_p = 5 \times 10^{-6} m_p c^2 \simeq 5$ keV in the following. Panel "a" of Figure 2 shows the temperature profiles for $M = 34 M_\odot$, $C_1 = 0.2$, $\beta_p = 1$, and $\beta_\nu = 3$. The critical mass accretion rate $\dot{M}_{\mathrm{cr}} = 21.9 L_{\mathrm{Edd}}/c^2$, which is consistent with equation (28). Therefore, if the hot accretion flow develops naturally with the processes considered here, a very high viscosity is needed to produce a hard X-ray luminosity on the order of $0.1 L_{\mathrm{Edd}}$. This statement is not necessarily true if the formation of hot accretion flows is triggered by some instability near black holes.

However, for $\dot{M} \sim \dot{M}_{\mathrm{cr}}$, the electron temperature is more than 1 MeV near the black hole, which is much higher than the observed values in the low-hard states (See Fig. 2 a). It is clear that, besides the local internal cooling processes considered above, other cooling processes have to be introduced to bring the electron temperature to the desired energy range. Observations of X-ray binaries in the low-hard states show that photons from the large-scale optically thick slim disk can provide sufficient soft photons to cool electrons in the inner two-temperature flow through IC (Barrio et al. 2003). The cooling rate will also increase if we consider a global radiation transfer and include the cooling due to pair production. Here we treat these cooling processes approximately by assuming the energy density of the soft photons produced outside the two-temperature accretion flow is three times higher than the local magnetic field energy density so that there is an extra cooling term 3 times higher than that given by equation (30). Panel "b" of Figure 2 shows the temperature profiles with this cooling effect included. In this case, $\dot{M}_{\mathrm{cr}} = 0.933 L_{\mathrm{Edd}}/c^2$, which is clearly affected by this extra cooling process. The other model parameters are the same as Panel "a".

According to this model, the IC of the external soft photons dominates the cooling, and the electron temperature is nearly constant at small radii due to the balance between Coulomb collisional heating and this cooling for $\dot{M} = \dot{M}_{\mathrm{cr}}$. The value of the electron temperature depends on the ratio of the external photon energy density to that of the magnetic field η:

$$k_{\mathrm{B}}T_e \simeq \left(\frac{9 \ln \lambda m_e}{4\sqrt{2\pi}\beta_p \eta m_p} \right)^{2/5} m_e c^2 . \tag{38}$$

The electron heating by turbulence becomes relatively more important for lower values of $\dot{M}$. However, with $\dot{M}$, which is proportional to the Thomson optical depth of the accretion flow,

varying by two orders of magnitude, the electron temperature in the inner region remains about 30 keV. This is not consistent with the recently observed anti-correlation between the electron temperature and the Thomson optical depth of Cygnus X-1 in the low-hard and intermediate states (Wilms et al. 2006; Titarchuk 1994).

By increasing the electron heating rate by one order of magnitude, i.e. with $C_1 = 0.02$, we obtain temperature profiles in Panel "c". Because IC cooling is already important at the outer boundary, $\dot{M}_{\mathrm{cr}} = 0.891 L_{\mathrm{Edd}}/c^2$ decreases slightly due to more efficient electron heating, which results in more cooling of the accretion flow. The other model parameters are the same as Panel "b". We see that the electron temperatures are in the observed energy range. Panel "d" shows profiles of the Thomson optical depth $\tau = 2\sigma_T H n$ and ε for the same models in Panel "c". We qualitatively recover the observed anti-correlation between $k_{\mathrm{B}}T_e$ and τ. The radiation efficiency of the accretion flow is ~ 0.01 giving rise to a luminosity of $\sim 10^{35-38}$ erg s^{-1}, which is also in line with observations. We note that $C_1\beta_\nu\beta_p = 0.06$ implying very efficient electron heating by turbulence.

6.   Conclusions and Discussion

To explain the millimeter and sub-millimeter spectrum and polarization of Sagittarius A* and the recently observed anti-correlation between the electron temperature and the Thomson optical depth of Cygnus X-1 in the low-hard and intermediate states, we show that electrons need to be heated efficiently by turbulence plasma waves. Coulomb collisions are not effective enough to heat electrons to the temperature required by observations of Sagittarius A* that has a very low accretion rate.

The critical mass accretion rate, below which a two-temperature solution may exist, is determined by the radiative cooling and Coulomb collisional heating processes and is almost independent of the electron heating by turbulence. To reproduce the observed high luminosity of X-ray binaries in the low accretion states, a high viscosity is required to increase the critical mass accretion rate, and the radial velocity of the accretion flow can be comparable to the Keplerian velocity. We show that the electron cooling for galactic X-ray binaries needs to be dominated by IC of an external soft photon field originated presumably from a large-scale cold slim disk. Synchrotron, synchrotron self-Comptonization, and bremsstrahlung processes inside the hot accretion flows are not efficient enough to cool the electrons to the observed temperature range. Assuming that the energy density of these external photons is 3 times higher than the local magnetic field energy density, we find that the electron temperature at the critical accretion rate is determined by this energy density ratio. A lower external photon energy density gives rise to a higher electron temperature. This high external photo

energy density suggests that the radiation field may have important dynamical effects and may be partially responsible for the required high viscosity.

Recent observations of Cygnus X-1 show that the electron temperature in the IC model (Titarchuk 1994) decreases by more than a factor of 10 when the Thomson optical depth, which is proportional to the accretion rate, increases by two orders of magnitude in the low-hard and intermediate states. We show that very efficient electron heating by turbulence can reproduce such an anti-correlation. Without this extra heating process (besides the Coulomb collisional heating), the electron temperature is almost independent of the accretion rate. It appears that such an anti-correlation may also be explained by adjusting the properties of the external photo field (Esin et al. 1998). It is, however, not clear whether the observed dramatic changes in both the electron temperature and the Thomson optical depth can be reproduced in such a scenario. Detailed modeling of the external photo field is required to address this issue and to fit the broadband spectrum of Cygnus X-1 in the low-hard and intermediate states.

We have shown that a two-temperature flow can develop self-consistently at small radii for low accretion rates mostly due to the fact that electrons and protons reach a thermal equilibrium with themselves much faster than with each other through Coulomb collisions. However, at very low accretion rates, there is no guarantee that the proton distribution is Maxwellian although electrons may reach a quasi-thermal distribution due to balancing between the cooling and heating processes. Observations of the low-hard states of X-ray binaries also suggest that the electron distribution is dominated by a thermal component. When Coulomb collision time scales are much longer than other relevant time scales, the particle "temperature" should be interpreted as a measurement of the internal energy but not a thermal distribution.

With the pseudo-Newtonian potential and assumption of Keplerian azimuthal velocities, processes below $\sim 3r_S$ can not be described accurately by our model. These processes can have important observational consequences (Titarchuk & Fiorito 2004) and may drive strong outflows responsible for the observed radio emission (Heinz & Sunyaev 2003; Fender et al. 2004; Falcke et al. 2004). By dropping these assumptions and considering the momentum conservation in the radial direction, one may build a more complete model to study these processes (Popham & Gammie 1998).

In the model we have ignored the vertical structure of the disk, dynamical effects of the radiation field, winds and/or outflows, outwardly directed waves, and pair productions, which can be important for X-ray binaries. These may introduce a factor of a few changes in our model parameters, especially in regards to the temperature profile of protons and the transition from an one-temperature flow at large radii to the two-temperature inner

region, which may have important implications on the origin of quasi-periodic oscillations. But our conclusion of the presence of efficient collision-less electron heating by turbulence is not affected. Electrons can also be accelerated by MHD turbulence to very high energies in coronas of the disk and produce the observed non-thermal high energy spectral component (Gierliński et al. 1999). These electrons carry much less energy than the thermal electron population considered in this paper and can be treated with appropriate corona models (Dermer et al. 1996; Li & Miller 1997).

Our treatment of the electron heating by turbulence is different from that proposed in the advection dominated accretion flow models (Yuan et al. 2006), where the energy equation is separated into two equations, one for electrons and the other for ions, and it is assumed that a fixed fraction of the viscously dissipated energy is deposited into electrons. We point out that equation (11) is the more appropriate energy equation one should adopt and there is no reasonable justification to split it into two equations except that the coupling between electrons and ions through plasma waves or turbulence can be ignored. Our results and the MRI clearly show the opposite, i.e. turbulence plays crucial roles in an accretion flow. It is also difficult to understand why a fixed fraction of the viscously dissipated energy goes into electrons. Electron heating by plasma waves should depend on the properties of the plasma and turbulence (Bisnovatyi-Kogan & Lovelace 1997; Quataert 1998). Equation (15) is perhaps more appropriate to describe the temperature evolution of electrons.

It is very challenging to study turbulence, one of the commonest natural phenomena. It originates from the non-linear nature of complex many body systems. In astrophysics, MHD turbulence is ubiquitous, and one of the most important effects of it is the energization of charged particles in collision-less plasmas. The microscopic details of this stochastic particle acceleration process are still a matter of debate. Even the common practice of treating MHD turbulence as a spectrum of plasma waves is not well justified, especially for strong turbulence. The results in this paper provide a means to study the energization of electrons and ions by turbulence, specifically the energy partition between the two particles, with observations. Our results suggest that the electron heating time by turbulence is at least 10 times shorter than that of protons at a given mean particle speed. Detailed modeling of the radiation spectrum and MHD simulations of the accretion flows will lead to more quantitative results.

We note that the dimensionless parameter C_1, which characterizes the electron heating by turbulence in our model, decreases by a factor of > 50 from the supermassive black hole of Sagittarius A* to the stellar mass black hole in Cygnus X-1. This may be related to the dramatic increase of the turbulence viscosity described by β_ν, which changes from 0.1 for Sagittarius A* to 3 for galactic X-ray binaries. Indeed, the product of the two changes by

less than a factor of 2. Because $\beta_\nu > 2C_2/3$ is proportional to the energy dissipation rate of MHD turbulence, the energy partition between electrons and ions is described by C_1C_2. Our results suggest that in the two-temperature accretion states of black holes, this partition weakly depends on the black hole mass and mass accretion rate.

REFERENCES

Agol, E., & Krolik, J. H. 2000, 528, 161

Aitken, D. K., Greaves, J., Chrysostomou, A., Jenness, T., Holland, W., Hough, J. H., Pierce-Price, D., & Richer, J. 2000, ApJ, 534, L173

Baganoff, F. K., et al. 2001, Nature, 413, 45

Balbus, S. A., & Hawley, J. F. 1991, ApJ, 555, L83

Barrio, F. E., Done, C., & Nayakshin, S. 2003, MNRAS, 342, 557

Bisnovatyi-Kogan, G. S., & Lovelace, R. V. 1997, ApJ, 486, L43

Bittner, J., Liu, S., Fryer, C. L., & Petrosian, V. 2007, ApJ, 661, 863

Blandford, R. D., & Begelman, M. C. 1999, MNRAS, 303, L1

Blandford, R., & Eichler, D. 1987, Phys. Report, 154, 1

Camenzind, M. 2005, MmSAI, 76, 98

Dermer, C. D., Miller, J. A., & Li, H. 1996, ApJ, 456, 106

Esin, A. A., Narayan, R., Cui, W., Grove, J. E., & Zhang, S. N. 1998, ApJ, 505, 854

Falcke, H., Körding, E., & Markoff, S. 2004, A&A, 414, 895

Fender, R. P., Belloni, T. M., & Gallo, E. 2004, MNRAS, 355, 1105

Genzel, R. et al. 2003, Nature, 425, 934

Ghez, A. M., et al. 2005, ApJ, 620, 744

Gierliński, M., & Done, C. 2004, MNRAS, 329, 7

Gierliński, M., et al. 1999, MNRAS, 309, 496

Gillessen S., et al. 2006, ApJ, 640, 163L

Hawley, J. F., & Balbus, S. A. 2002, ApJ, 573, 738

Heinz, S., & Sunyaev, R. A. 2003, MNRAS, 343, L59

Li, H., & Miller, J. A. 1997, 478, L67

Liu, S., & Melia, F. 2002, ApJ, 566, L77

Liu, S., Melia, F., Petrosian, V., & Fatuzzo, M. 2006a, ApJ, 647, 1099

Liu, S., Petrosian, V., Melia, F., & Fryer, C. L. 2006b, ApJ, 648, 1020

Liu, S., Qian, L., Wu, X.-B., Fryer, C. L., & Li, H. 2007, ApJ, submitted, arXiv: 0705.2792.

Mahadevan, R., Narayan, R., & Yi, I. 1996, ApJ, 465, 327

Melia, F., & Coker, R. 1999, ApJ, 511, 750

Melia, F., Liu, S., & Coker, R. 2000, ApJ, 545, L117

Melia, F., Liu, S., & Coker, R. 2001, ApJ, 553, 146

Meyer-Hofmeister, E., Liu, B. F., & Meyer, F. 2005, A&A, 432, 181

Narayan, R., & Yi, I. 1995, ApJ, 452, 710

Paczyńsky, B., & Wiitta, P. J. 1980, A&A, 88, 23

Pessah, M. E., Chan, C. K., & Psaltis, D. 2006, PRL, 97, 221103

Petrosian, V. 1981, ApJ, 251, 727

Popham, R., & Gammie, C. F. 1998, ApJ, 504, 419

Quataert, E. 1998, ApJ, 500, 978

Quataert, E., & Gruzinov, A. 2000, ApJ, 545, 842

Readhead, A. C. S. 1994, ApJ, 426, 51

Rees, M. J., Begelman, M. C., Blandford, R. D., & Phinney, E. S. 1982, Nature, 295, 17

Remillard, R. A., Morgan, E. H., McClintock, J. E., Bailyn, C. D., & Orosz, J. A. 1999, ApJ, 522 397

Rybicki, G., & Lightman, A. 1979, Radiative Processes in Astrophysics (New York: Wiley)

Schödel, R., et al. 2002, Nature, 419, 694

Shakura, N. I., & Sunyaev, R. A. 1973, A&A, 24, 337

Shapiro, S. L., Lightman, A. P., & Eardley, D. M. 1976, ApJ, 204, 187

Sharma, P., Quataert, E., Hammett, G. W., & Stone, J. M. 2007, ApJ, submitted, astro-ph/0703572

Shen, Z. Q., Lo, K. Y., Liang, M. C., Ho, P. T. P., & Zhao, J. H. 2005, Nature, 438, 62

Spitzer, L. S. 1962, Physics of Fully Ionized Gases, (Dover Publications, Inc. Mineola, New York)

Titarchuk, L. 1994, ApJ, 434, 570

Titarchuk, L., & Fiorito, R. 2004, ApJ, 612, 988

Wilms, J., Nowak, M. A., Pottschmidt, K., Pooley, G. G., & Fritz, S. 2006, A&A, 447, 245

Wolfe, B., & Melia, F. 2006, ApJ, 638, 125

Yuan, F., Taam, R. E., Xue, Y., & Cui, W. 2006, ApJ, 636, 46

Zdziarski, A. A., Poutanen, J., Paciesas, W. S., & Wen, L. Q. 2002, ApJ, 578, 357
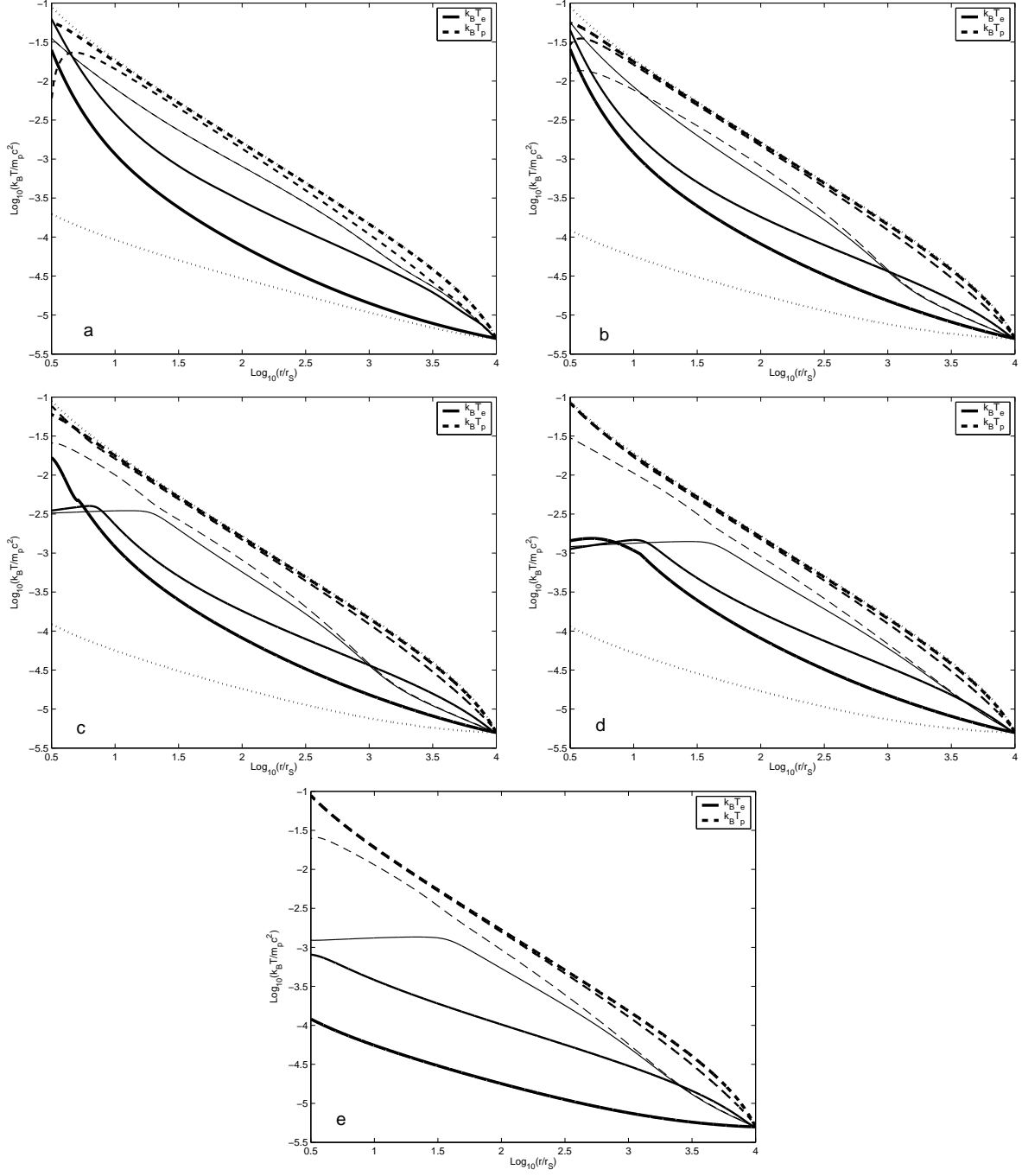
Zhang, S. N., et al. 2000, Science, 287, 1239

Fig. 1.— a: Temperature profiles of electrons (solid) and protons (dashed) for $\dot{M} = 10^{-7}$ (thick), 10^{-3} (medium), 10 (thin) L_{Edd}/c^2. Cooling is not included to demonstrate the effects of electron heating by turbulence and Coulomb collisions. The electron and proton temperatures at the outer boundary are chosen so that $k_{\mathrm{B}}T_e = k_{\mathrm{B}}T_p$ is equal to 1/10 of the gravitational binding energy of protons and $\varepsilon < 0$. $C_1 = 1.5$, $\beta_\nu = 0.1$, and $\beta_p = 1$. The dotted lines have $C_1 = 15$ and $\dot{M} = 10^{-5} L_{\mathrm{Edd}}/c^2$. Note that the proton temperature decreases sharply toward small radii for $\dot{M} = 0.001 L_{\mathrm{Edd}}/c^2$ and the electron and proton temperatures are identical for $\dot{M} = 10 L_{\mathrm{Edd}}/c^2$. See text for details. b: Similar to "a" with the bremsstrahlung cooling included and $\dot{M} = 2.63 \times 10^{-6}$ (thick), 2.63×10^{-4} (medium), 2.63×10^{-2} (thin) L_{Edd}/c^2. The disk collapses to a cold disk at small radii for $\dot{M} > \dot{M}_{\mathrm{cr}} = 2.63 \times 10^{-2} L_{\mathrm{Edd}}/c^2 (r/10^4 r_{\mathrm{S}})^{-1/2}$. The dotted lines have $C_1 = 15$ and the same accretion rate as the thick lines. c: Same as "b" with all the cooling processes included and $M = 3.4 \times 10^6 M_\odot$. We see that the synchrotron and IC coolings only affect the temperature profile of electrons at small radii. d: Same as "c" but for $M = 3.4 M_\odot$. Because the synchrotron cooling time in the optically thick region scales as $M^{3/2}$, the electron temperature decreases with M and $\dot{M}_{\mathrm{cr}} = 2.13 \times 10^{-2} L_{\mathrm{Edd}}/c^2$. e: Same as "d" but for $C_1 = 15$. $\dot{M}_{\mathrm{cr}} = 2.51 \times 10^{-2} L_{\mathrm{Edd}}/c^2$
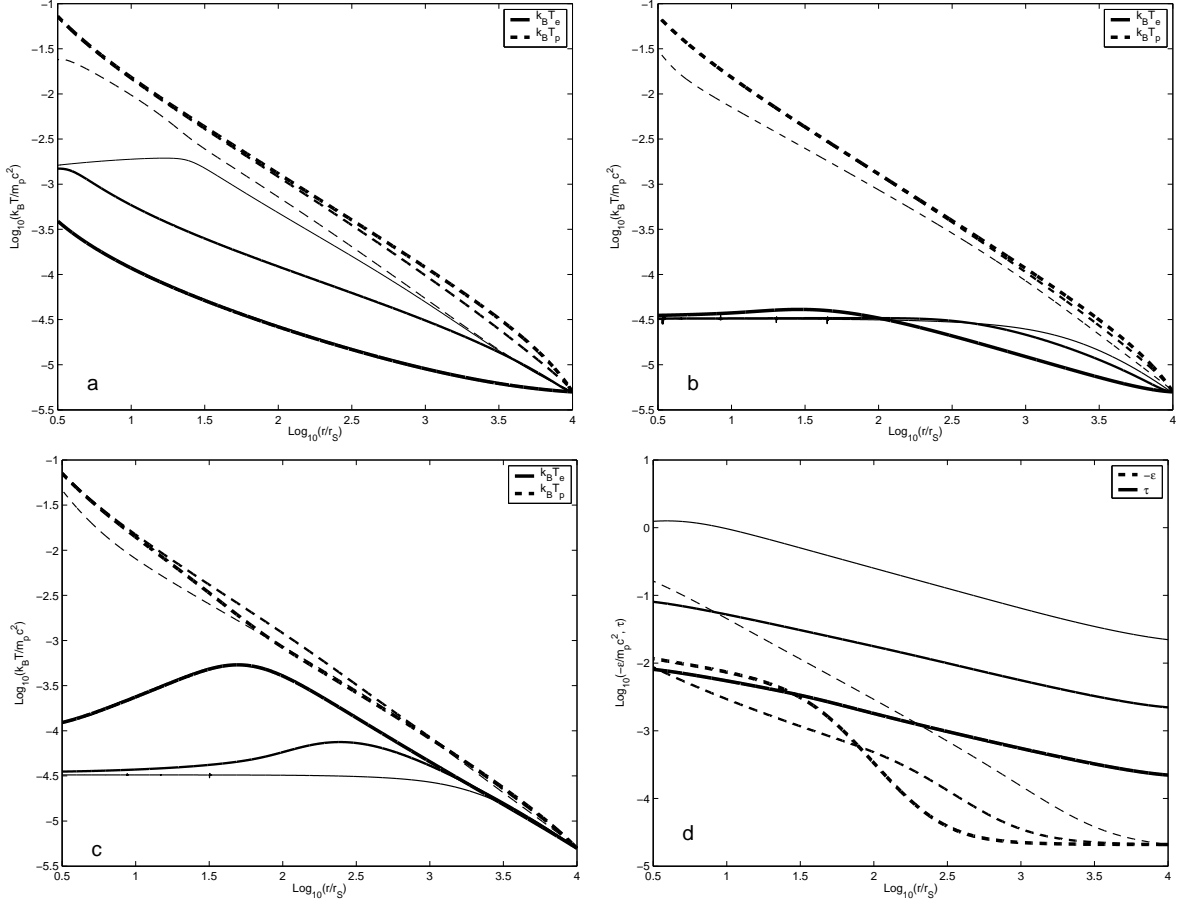
Fig. 2.— a: Same as "e" of Figure 1 but for $M = 34M_\odot$, $C_1 = 0.2$, $\beta_p = 1$, $\beta_\nu = 3$ and $\dot{M} = 2.19 \times 10^{-3}$ (thick), 0.219 (medium), 21.9 (thick) L_{Edd}/c^2. In this case, $\dot{M}_{\mathrm{cr}} = 21.9L_{\mathrm{Edd}}/c^2$. b: Same as "a" but with an external soft photo field, whose energy density is 3 times higher than the local magnetic field energy density. $\dot{M} = 9.33 \times 10^{-3}$ (thick), 9.33×10^{-2} (medium), 0.933 (thin) L_{Edd}/c^2, and $\dot{M}_{\mathrm{cr}} = 0.933L_{\mathrm{Edd}}/c^2$. c: Same as "b" but for $C_1 = 0.02$, and $\dot{M} = 8.91 \times 10^{-3}$ (thick), 8.91×10^{-2} (medium), 0.891 (thin) L_{Edd}/c^2. $\dot{M}_{\mathrm{cr}} = 0.891L_{\mathrm{Edd}}/c^2$. d: Profiles of ε (dashed) and τ (solid) for the three models in "c". The thickness of the lines are the same for a given accretion rate. The luminosity of the disk for the thin lines is more than 9% of L_{Edd}.